Investigating crystalline-polarity-dependent electronic structures of GaN by hard x-ray photoemission and *ab-initio* calculations

Takeo Ohsawa,[1,a)] Shigenori Ueda,[2,3] Motohiro Suzuki,[4] Yoshitaka Tateyama,[5,6] Jesse R. Williams,[5] and Naoki Ohashi[1,7]
[1]*National Institute for Materials Science (NIMS), 1-1 Namiki, Tsukuba, Ibaraki 305-0044, Japan*
[2]*Synchrotron X-ray Station at SPring-8, NIMS, Sayo, Hyogo 679-5148, Japan*
[3]*Quantum Beam Unit, NIMS, Sayo, Hyogo 679-5148, Japan*
[4]*Japan Synchrotron Radiation Research Institute (JASRI), Sayo, Hyogo 679-5198, Japan*
[5]*International Center for Materials Nanoarchitectonics (MANA), NIMS, 1-1 Namiki, Tsukuba, Ibaraki 305-0044, Japan*
[6]*PRESTO, Japan Science and Technology Agency (JST), 4-1-8 Honcho, Kawaguchi, Saitama 333-0012, Japan*
[7]*Materials Research Center for Element Strategy (MCES), Mailbox SE-6, Tokyo Institute of Technology, 4259 Nagatsuta, Midori-ku, Yokohama 226-0026, Japan*

(Received 7 June 2015; accepted 18 October 2015; published online 30 October 2015)

Crystalline-polarity-dependent electronic structures of gallium nitride (GaN) were studied by photoemission spectroscopy (PES) using soft and hard x-rays with different linear polarizations. A peak located near the valence band (VB) maximum was enhanced for a (0001) surface compared with that for a $(000\bar{1})$ surface regardless of photon energy. Comparison of the VB density of states obtained by *ab-initio* calculations with the observed VB-PES spectra indicates that the crystalline-polarity dependence is associated with the Ga 4*p* and N 2*p* states. The most plausible origin of the crystalline-polarity-dependent VB feature is based on the photoemission phenomena of electrons in the p_z-orbitals due to spontaneous electric polarization along the *c*-axis of GaN.
 [http://dx.doi.org/10.1063/1.4934842]

Gallium nitride (GaN) crystallizes to form a wurtzite (WZ)-type structure consisting of alternating Ga (cation) and N (anion) layers stacked along the *c*-axis. Hence, its spontaneous electric polarization appears along *c*-axis,[1,2] and the polar structure is responsible for the piezoelectric and pyroelectric properties of GaN. In terms of practical applications, the crystalline polarities of WZ-type semiconductors affect their surface morphologies[3] and crystal qualities[4] during crystal growth, in addition to the energy efficiencies of light-emitting diodes.[5] As reviewed in earlier works,[6,7] the effects of the electric dipole induced by both spontaneous and piezoelectric polarization in WZ-type nitride semiconductors are important for further development of the optoelectronic devices based on these semiconductors.[8,9] In this context, the determination of the crystalline polarity of WZ-type semiconductors is an essential first step in achieving an understanding of the fundamental physical and chemical phenomena resulting from the crystalline polarity.

The crystalline polarity of WZ-type crystals has been determined by surface morphology investigations after chemical etching,[10] ion scattering spectroscopy,[11] convergent beam electron diffraction,[12] and x-ray diffraction.[13] Recently, several groups have investigated the polar surfaces of WZ-type semiconductors by means of photoemission spectroscopy (PES).[14–16] In particular, it was reported in our previous work that the peak at ~5 eV in the binding energy (E_B) was enhanced for the (0001) face of ZnO compared with that of the $(000\bar{1})$ face.[17] Our results of angle-resolved hard x-ray PES (AR-HXPES) studies on ZnO have indicated that neither the orientation of the surface facets nor the surface contamination generates the crystalline-polarity dependence of valence band (VB) spectra, but that the crystalline polarity along the *c*-axis is the real origin of the crystalline-polarity-dependent VB-HXPES profile.[17] In particular, the crystalline-polarity dependence of the VB-HXPES profiles originates not from the surface orientation but from the angle defined by the $\langle\overrightarrow{0001}\rangle$ axis of the WZ-type lattice and the photoelectron trajectory ($\vec{\nu_e}$).[17] Therefore, one can determine the crystalline polarity of a WZ-type semiconductor from the VB-PES spectral shape. The effectiveness of the PES technique for the crystalline-polarity determination of WZ-type lattices was confirmed by an AR-PES study on GaN[18] following our AR-HXPES study on ZnO.[17]

VB-PES profiles are useful indicators of the crystalline polarities of WZ-type semiconductors as mentioned earlier, although the reason why the spectroscopic features depend on the crystalline polarity is still under debate. Thus, we were motivated to study the polar GaN semiconductors by the HXPES, especially using linearly polarized x-rays. Since the per electron photoionization cross-section (σ) depends on the photon energy ($h\nu$) and angular momenta of the electrons (*s, p, d,* or *f*),[19–22] the VB profiles measured with soft x-ray PES (SXPES) and HXPES should be different from each other. Indeed, in the HXPES spectra, the σ-values of the *s*-orbitals are relatively larger than those of the *p*- and *d*-orbitals except in heavy elements such as 5*d* transition metals. Furthermore, the use of linearly polarized x-rays with different electric vector ($\vec{E}$) directions provides further detailed information because the σ-values also depend on the experimental geometry (i.e., the relationship between the x-ray propagation direction, $\vec{E}$, and $\vec{\nu_e}$).[20–22] Thus, we can extract

[a)]Electronic mail: ohsawa.takeo@nims.go.jp

the local and partial density-of-states (DOS) by utilizing the $\vec{E}$ and $h\nu$ dependences of σ-value of the atomic orbitals. In fact, Sekiyama *et al.* demonstrated that linear dichroism in the HXPES is a useful technique for experimental characterization of the electron orbitals in Ag and Au.[23] Thus, in this study, we utilized the HXPES with linearly polarized x-rays to analyze the electronic structures of the polar surfaces of GaN.

We characterized commercially available GaN single crystals with well-polished Ga-face (0001) and N-face ($000\bar{1}$) without any specific surface treatments. Our preliminary studies indicated that surface treatments, such as ion sputtering and scratching, did not change the crystalline-polarity dependence of the HXPES spectra. The HXPES and SXPES measurements were performed at the revolver undulator beamline BL15XU of SPring-8, Japan. The instrumental setup at BL15XU has been described later.[24] Two different x-ray photon energies, $h\nu = 2$ keV (soft x-ray) and 6 keV (hard x-ray), were used. All of the measurements were performed by the near-normal emission geometry, where the incidence angle of the x-rays and take-off angle of the photoelectrons were set to 1° and 89° (acceptance angle of ±7°), respectively, relative to the GaN surface (see the supplementary material[25]). For the HXPES measurements, we used two different linearly polarized x-rays, for which $\vec{E}$ was parallel (horizontally linearly polarized: E(H)) or perpendicular (vertical linearly polarized: E(V)) to $\vec{\nu}_e$ of the analyzer. The E(V)-x-rays were obtained with a diamond phase retarder: the 6 keV x-rays from the undulator were E(H)-x-rays with a degree of linear polarization (P) of ∼1.00, while P for E(V)-x-rays was estimated to be ∼0.70. It should also be noted that P for 2 keV x-rays was estimated to be ∼0.94. The total energy resolution was set to about 145 meV, and E_B was referred to the Fermi level (E_F) of an evaporated Au film.

Furthermore, we calculated the total DOS and projected-DOSs (PDOSs) for "bulk" GaN by using *ab-initio* calculations based on density functional theory (DFT). A pseudopotential DFT code called CASTEP[26] was used. The norm-conserving-pseudo-potentials (NCPPs) generated by OPIUM code[27] were adopted in these calculations. We performed several calculations by using different exchange functions, such as a local density approximation (LDA),[28] and NCPPs constructed with different conditions. As a result, a combination of the screened-exchange (sX-LDA) function[29] and NCPPs constructed by using the LDA function provided the best consistency between the observed and calculated VB widths.[25] Mulliken population analyses of the DFT calculation results were used for the PDOS.[30,31]

The crystalline-polarity dependences of the HXPES and SXPES spectra in the VB region at room temperature are shown in Figure 1. All of the spectra shown here were measured with E(H)-x-rays. For convenience, four spectral features, P_1 through P_4, are indicated in the figure. The P_1 peak is enhanced for the (0001) face compared to that of the ($000\bar{1}$) face. This feature is very similar to those observed for the polar surfaces of ZnO[14,15,17] and GaN.[18] Thus, the relative intensity of P_1 is a fingerprint for the (0001) face, that is, the cation-polar surface of a WZ-type lattice. In addition, the crystalline-polarity dependence of the P_1 peak

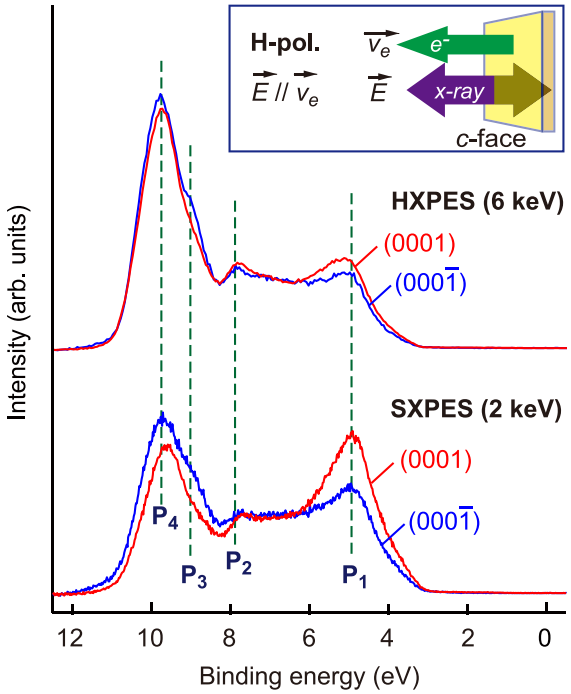

FIG. 1. Valence band HXPES and SXPES spectra for (0001) and ($000\bar{1}$) surfaces of GaN measured with E(H)-x-rays.

intensity is more significant in the SXPES than in the HXPES. This difference is discussed later.

Figure 2 compares the HXPES spectra in the VB region measured with E(H)-x-rays [E(H)-HXPES)] and E(V)-x-rays [E(V)-HXPES] for the (0001) and ($000\bar{1}$) faces of GaN. Here, the E(V)-HXPES spectra have been corrected to $P \sim 1.00$ by using the HXPES intensity ratios for E(V) ($P \sim 0.70$) and E(H) ($P \sim 1.00$) x-rays. The spectra were normalized by the photon flux. Remarkably, the relative intensities of the

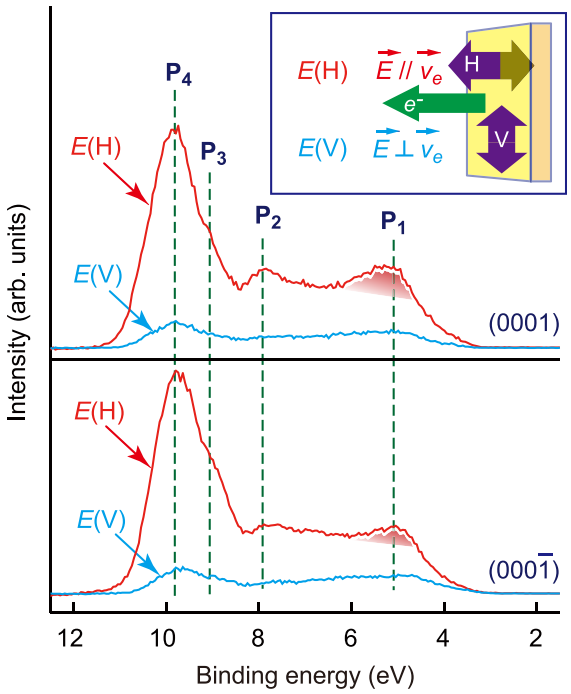

FIG. 2. Valence band HXPES spectra for (0001) and ($000\bar{1}$) surfaces of GaN measured with 6 keV E(H)- and E(V)-x-rays.

TABLE I. Per electron cross-sections (σ) for valence orbitals of GaN with 6 keV E(H)- and E(V)-x-rays in our experimental geometry according to data from J. H. Scofield, California University, Livermore, Lawrence Livermore Laboratory, Technical Report No. UCRL-51326 (1973); Trzhaskovskaya *et al.*, At. Data Nucl. Data Tables **77**, 97–159 (2001); Trzhaskovskaya *et al.*, At. Data Nucl. Data Tables **92**, 245–304 (2006); and J. Yeh and I. Lindau, At. Data Nucl. Data Tables **32**, 1–155 (1985). For comparison, σ-values for 2 keV E(H)-x-rays are also listed. Units of σ are barns.

		Cross section (σ)			
Element	Orbital	E(H) (6 keV)	E(V) (6 keV)	E(H) (2 keV)	E(V) (2 keV)
N	2*s*	29.8	0.602	770	9.15
	2*p*	0.134	0.123	12.5	8.21
Ga	4*s*	99.8	1.03	1011	8.27
	4*p*	11.5	2.53	287	33.6
	3*d*	10.9	5.63	963	296

E(H)-HXPES spectra are higher than those of the E(V)-HXPES spectra regardless of the crystalline polarity. This difference results from the σ-values of the E(H)-x-rays being higher than those of the E(V)-x-rays for all of the electron orbitals, as shown in Table I in our experimental geometry. The intensities of P_3 and P_4 measured with E(V)-x-rays are strongly suppressed compared with those of P_1 and P_2. The suppression of the P_3 and P_4 intensities strongly suggests that these structures involve *s*-orbital-like characteristics, and this idea is also supported by the x-ray polarization dependence of the σ-values. It is remarkable to note that negligible crystalline-polarity dependence of the intensities of P_1 and P_2 in the E(V)-HXPES spectra is observed, in contrast to that observed in the E(H)-HXPES results as shown in Figure 1. Therefore, we can conclude that the crystalline-polarity dependence appears when $\vec{E}$ is parallel to $\vec{\nu}_e$.

Figure 3 shows the PDOS profiles for "bulk" WZ-type GaN obtained by the DFT calculations,[25] where the energies are referred relative to the VB maximum (VBM). The calculated total DOS is also shown in Figure 3. We see that the four structures, P_1-P_4, in the observed HXPES and SXPES spectra are clearly identifiable in the calculated PDOS and total DOS profiles. By comparing the total DOS profile with the PDOSs in detail, the lower-energy part (~1–3 eV) of the VB, that is, the P_1 structure, is observed

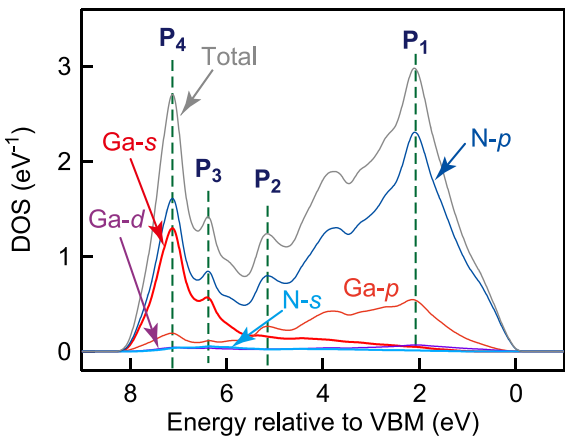

FIG. 3. PDOSs in valence band of "bulk" GaN. Energies are referred relative to the valence band maximum.

to arise primarily from the N 2*p* and Ga 4*p* states, while the higher-energy part (~6–8 eV) is dominated by the N 2*p* and Ga 4*s* states. Considering the variation between the σ-values of 6 keV E(H)- and E(V)-x-rays, as listed in Table I, one might assume that the contribution of the Ga 4*s* states to the E(V)-HXPES spectra would be strongly suppressed, because the σ-value for the Ga 4*s* orbital is almost zero in our experimental geometry. In fact, in the VB spectra for both the (0001) and (000$\bar{1}$) faces, the intensity ratio of P_4 in the E(V)-HXPES spectrum to that in the E(H)-HXPES spectrum is significantly lower than the corresponding ratios of P_1 and P_2. Therefore, we can conclude that P_4 in the E(H)-HXPES spectra is mainly attributable to the Ga 4*s* states. Returning back to Figure 1, the P_3 and P_4 structures decrease as P_1 increases on the (0001) face. Such spectral weight transfer from P_3 and P_4 to P_1 indicates that P_1 non-negligibly contains the Ga 4*s* state. On the other hand, the P_1 structure, which is composed of the N 2*p* and Ga 4*p* states in the PDOSs, reflects the Ga 4*p* state because its σ-value is larger than that of N 2*p*. In addition, significantly high intensity of P_1 in the SXPES spectrum for the (0001) surface can be also explained by the σ-values. The ratios of σ(N 2*p*)/σ(N 2*s*) and σ(N 2*p*)/σ(Ga 4*p*) are larger in the E(H)-SXPES than those in the E(H)-HXPES as shown in Table I. As the P_1 structure mostly consists of the N 2*p* orbital, the P_1 peak should be enhanced in the E(H)-SXPES than in the E(H)-HXPES. Hence, it is reasonable to attribute the origin of P_1 to the electronic structures composed of N 2*p* and Ga 4*p*.

Figure 4 compares the observed and calculated VB-HXPES spectra. The calculated spectra were obtained by the sum of the PDOSs weighted with the σ-values as given in Table I. Note that the present PDOSs are not for "surface" but for "bulk," and thus, the crystalline-polarity dependence was not considered in the DFT calculations for simplicity. The calculated E(H)- and E(V)-HXPES spectra show significant differences in their spectral shapes and intensities. As all the σ-values of the E(H)-x-rays are larger than those of the E(V)-x-rays in our experimental geometry, the calculated intensity of the E(H)-HXPES spectrum is much higher in the whole energy range than that for the E(V)-HXPES spectrum, as shown in the bottom panel in Figure 4. This trend is qualitatively in accordance with the observed spectra. As shown in the middle panel of Figure 4, the significant $\vec{E}$ dependence of the calculated intensities of P_3 and P_4 is due to the fact that the σ-value of the *s*-orbital for E(V)-x-rays with $P = 1.00$ is strongly suppressed in the dipole approximation. In the calculated E(V)-HXPES spectrum, P_3 and P_4 can be identified, but their intensities are considerably lower than those in the calculated E(H)-HXPES spectrum. Indeed, the $\vec{E}$ dependences of the calculated and observed spectra closely agree with the (000$\bar{1}$) surface. As the observed and calculated spectra for E(V) are in very good agreement across the entire VB range including P_1-P_4, we can conclude that the observed VB spectra, including the $\vec{E}$ dependence, were well reproduced by the simulation. However, since the photohole lifetime broadening effects were not included in the simulation, the intensities of P_3 and P_4 are emphasized in the calculated E(H)-HXPES spectrum.

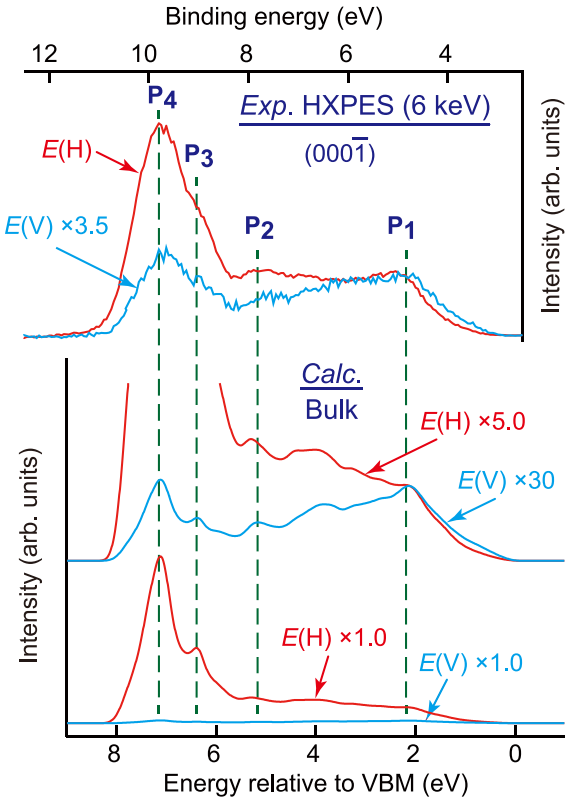

FIG. 4. Comparison of observed and calculated valence band HXPES spectra of GaN. (Top) Observed E(H)- and E(V)-HXPES spectra for GaN(000$\bar{1}$) face. (Middle and bottom) Calculated E(H)- and E(V)-HXPES spectra for "bulk" GaN.

Finally, we discuss the origin of the crystalline-polarity dependence of the P_1 intensity. It should be noted that the polarity dependence is a common feature in the WZ-type semiconductors,[14,15,17,18] and in particular, the P_1 peak is highly enhanced for (0001) surface of InN.[32] From the viewpoint of σ-values, it is reasonable to conclude that P_1 peak was enhanced when σ(O or N 2p) and σ(metal p) take large values. Indeed, σ(In 5p)/σ(In 5s) ratio, i.e., 0.44, is much higher than σ(Ga 4p)/σ(Ga 4s), i.e., 0.28, for E(H)-SXPES (2 keV)[19,20] and such difference in σ should be the most probable reason for the huge enhancement of P_1 peak for InN. Moreover, a consistency between the P_1 intensity and $\sigma(p)$-values supports our conclusion that the P_1 peak consists of metal p_z and anion p_z orbitals. It has been reported that there was negligible crystalline-polarity dependence in the VB spectra of ZnO when vacuum-ultraviolet-PES (VUVPES) are employed.[15] As σ(Zn 4p) and σ(O 2p) are much lower than σ(Zn 3d) with VUV, there is a possibility that the VUVPES is not an appropriate probe for detecting the polarity-dependent VB spectra because of its relatively low sensitivity to p-states. For example, the relatively weak P_1 features in the HXPES and VUVPES compared with those in the SXPES do not result from the difference in probing depth,[33] but from the excitation-energy dependence of σ-values.

It is of importance to note that the calculated and observed VB spectra were in good agreement for the (000$\bar{1}$) face. As the calculated spectra were obtained from the PDOSs for "bulk" GaN, it is presumable that the spectra obtained from the (000$\bar{1}$) face, where the P_1 feature was less obvious, may be closer to the electronic structure of "bulk" GaN. Assuming that the electronic state generating the P_1 structure is expressed by a linear combination of atomic orbitals as $\Psi = \alpha \cdot \text{Ga } 4p_z + (1-\alpha) \cdot \text{N } 2p_z$, where α is a function of the local atomic arrangements, the difference between the P_1 features of the (0001) and (000$\bar{1}$) faces indicates different α-values in these surface regions. If α at the topmost (0001) surface significantly differs from that in the bulk, the crystalline-polarity-dependent VB-HXPES spectra should be more obvious if surface-sensitive measurements were performed. However, as noted in our previous report,[17] the polarity dependence was more obvious when bulk-sensitive measurements (normal emission) were used. Therefore, it is not reasonable to attribute the crystalline-polarity-dependent VB-HXPES profile to variations in α caused by surface reconstructions, although the surface relaxation at the topmost surface is one of the most reasonable assumptions. These results indicate that the P_1 feature is not determined by α in the vicinity of GaN surfaces.

Here, it has to be reminded that the enhancement of P_1 peak was obvious when $\vec{\nu_e}$ was parallel to $\langle 000\bar{1} \rangle$ even for the facet not parallel to (0001) face.[17,18] Based on the results of the DFT calculations, it is reasonable to speculate that p_z electrons interact with the spontaneous polarization of WZ-type lattices since those orbitals spread parallel to the polarization vector. Assuming that the spontaneous polarization and the orbital interact with each other during ionization processes, the result of interactions may be obviously seen when $\vec{\nu_e}$ is parallel to both the p_z orbital and the spontaneous polarization vector. Hence, we conclude that the P_1 structure is closely associated with the polarization-related photoemission phenomena of electrons in the p_z-orbitals of GaN. Towards full understanding of the P_1 structure, we should study the dynamics of photoionization in terms of the internal electric field.

In summary, we studied the electronic structures of polar GaN with the HXPES and SXPES. The peak located at $E_B \approx 5$ eV (P_1) was enhanced in the VB spectra of the (0001) face compared with those of the (000$\bar{1}$) face. It was confirmed that the observation of the P_1 intensity is a suitable method for determining the crystalline polarity in GaN. Remarkably, the E(H)- and E(V)-HXPES spectra are quite different in intensity and shape. The x-ray polarization-dependent VB-HXPES profiles were qualitatively consistent with the PDOSs obtained by the DFT calculations. Based on these results, we conclude that the P_1 structure of the (0001) face is associated with the polarization-related photoemission phenomena of electrons in the p_z-orbitals of GaN.

The authors appreciate the staff of HiSOR, Hiroshima University and JAEA/SPring-8 for the development of HXPES at BL15XU of SPring-8. The HXPES experiments were performed with the approval of the NIMS Synchrotron X-ray Station (Proposal Nos. 2010B4607, 2011A4610, 2011B4610, 2012A4603, 2012A4612, 2012B4612, and 2013A4716). The authors thank Dr. M. Sumiya of NIMS for providing the GaN single crystals used in this study. S.U. and N.O. acknowledge the support from the Tokodai Institute for Elemental Strategy (TIES), which has been funded by the Ministry of Education, Culture, Sports, Science and Technology (MEXT), Japan. Y.T.

was partially supported by KAKENHI (Grant No. 15K05138). This work was also supported by the Strategic Programs for Innovative Research (SPIRE), MEXT, and the Computational Materials Science Initiative (CMSI), Japan.

[1]F. Bernardini, V. Fiorentini, and D. Vanderbilt, Phys. Rev. B **56**, R10024–R10027 (1997).
[2]O. Ambacher, J. Smart, J. R. Shealy, N. G. Weimann, K. Chu, M. Murphy, W. J. Schaff, L. F. Eastman, R. Dimitrov, L. Wittmer, M. Stutzmann, W. Rieger, and J. Hilsenbeck, J. Appl. Phys. **85**, 3222–3233 (1999).
[3]A. R. Smith, R. M. Feenstra, D. W. Greve, M.-S. Shin, M. Skowronski, J. Neugebauer, and J. E. Northrup, Appl. Phys. Lett. **72**, 2114–2116 (1998).
[4]T. Hashimoto, F. Wu, J. S. Speck, and S. Nakamura, Nat. Mater. **6**, 568–571 (2007).
[5]I. Akasaki and H. Amano, Jpn. J. Appl. Phys., Part 1 **45**, 9001–9010 (2006).
[6]M. Feneberg and K. Thonke, J. Phys.: Condens. Matter **19**, 403201 (2007).
[7]V. Avrutin, S. D. A. Hafiz, F. Zhang, U. Ozgur, H. Morkoc, and A. Matulionis, J. Vac. Sci. Technol., A **31**, 050809 (2013).
[8]S. Choi, M.-H. Ji, J. Kim, H. Jin Kim, M. M. Satter, P. D. Yoder, J.-H. Ryou, R. D. Dupuis, A. M. Fischer, and F. A. Ponce, Appl. Phys. Lett. **101**, 161110 (2012).
[9]M. Okada, Y. Saitoh, M. Yokoyama, K. Nakata, S. Yaegassi, K. Katayama, M. Ueno, M. Kiyama, T. Katsuyama, and T. Nakamura, Appl. Phys. Express **3**, 054201 (2010).
[10]D. A. Stocker, E. F. Schubert, and J. M. Redwing, Appl. Phys. Lett. **73**, 2654 (1998).
[11]S.-K. Hong, T. Hanada, H.-J. Ko, Y. Chen, T. Yao, D. Imai, K. Araki, M. Shinohara, K. Saitoh, and M. Terauchi, Phys. Rev. B **65**, 115331 (2002).
[12]T. Mitate, S. Mizuno, H. Takahata, R. Kakegawa, T. Matsuoka, and N. Kuwano, Appl. Phys. Lett. **86**, 134103 (2005).
[13]H. Tampo, P. Fons, A. Yamada, K.-K. Kim, H. Shibata, K. Matsubara, S. Niki, H. Yoshikawa, and H. Kanie, Appl. Phys. Lett. **87**, 141904 (2005).
[14]N. Ohashi, Y. Adachi, T. Ohsawa, K. Matsumoto, I. Sakaguchi, H. Haneda, S. Ueda, H. Yoshikawa, and K. Kobayashi, Appl. Phys. Lett. **94**, 122102 (2009).
[15]M. W. Allen, D. Y. Zemlyanov, G. I. N. Waterhouse, J. B. Metson, T. D. Veal, C. F. McConville, and S. M. Durbin, Appl. Phys. Lett. **98**, 101906 (2011).
[16]T. Nakamura, T. Yoshimura, A. Ashida, and N. Fujimura, Thin Solid Films **559**, 88–91 (2014).
[17]J. Williams, H. Yoshikawa, S. Ueda, Y. Yamashita, K. Kobayashi, Y. Adachi, H. Haneda, T. Ohgaki, H. Miyazaki, T. Ishigaki, and N. Ohashi, Appl. Phys. Lett. **100**, 051902 (2012).
[18]D. Skuridina, D. V. Dinh, B. Lacroix, P. Ruterana, M. Hoffmann, Z. Sitar, M. Pristovsek, M. Kneissl, and P. Vogt, J. Appl. Phys. **114**, 173503 (2013).
[19]J. H. Scofield, California University, Livermore, Lawrence Livermore Laboratory, Technical Report No. UCRL–51326, 1973.
[20]M. Trzhaskovskaya, V. Nefedov, and V. Yarzhemsky, At. Data Nucl. Data Tables **77**, 97–159 (2001).
[21]M. Trzhaskovskaya, V. Nikulin, V. Nefedov, and V. Yarzhemsky, At. Data Nucl. Data Tables **92**, 245–304 (2006).
[22]J. Yeh and I. Lindau, At. Data Nucl. Data Tables **32**, 1–155 (1985).
[23]A. Sekiyama, J. Yamaguchi, A. Higashiya, M. Obara, H. Sugiyama, M. Y. Kimura, S. Suga, S. Imada, I. A. Nekrasov, M. Yabashi, K. Tamasaku, and T. Ishikawa, New J. Phys. **12**, 043045 (2010).
[24]S. Ueda, J. Electron Spectrosc. Relat. Phenom. **190**, 235–241 (2013).
[25]See supplementary material at http://dx.doi.org/10.1063/1.4934842 for detailed description of experimental conditions and results of simulations.
[26]S. J. Clark, M. D. Segall, C. J. Pickard, P. J. Hasnip, M. I. J. Probert, K. Refson, and M. C. Payne, Z. Kristallogr. **220**, 567–570 (2005).
[27]A. Rappe, K. Rabe, E. Kaxiras, and J. Joannopoulos, Phys. Rev. B **41**, 1227–1230 (1990).
[28]J. P. Perdew, Phys. Rev. B **23**, 5048–5079 (1981).
[29]R. Asahi, W. Mannstadt, and A. Freeman, "Optical properties and electronic structures of semiconductors with screened-exchange LDA," Phys. Rev. B **59**, 7486–7492 (1999).
[30]M. Segall, R. Shah, C. Pickard, and M. Payne, Phys. Rev. B **54**, 16317–16320 (1996).
[31]M. D. Segall, P. J. D. Lindan, M. J. Probert, C. J. Pickard, P. J. Hasnip, S. J. Clark, and M. C. Payne, J. Phys.: Condens. Matter **14**, 2717 (2002).
[32]T. Veal, P. King, P. Jefferson, L. Piper, C. McConville, H. Lu, W. Schaff, P. Anderson, S. Durbin, D. Muto, H. Naoi, and Y. Nanishi, Phys. Rev. B **76**, 075313 (2007).
[33]S. Tanuma, C. J. Powell, and D. R. Penn, Surf. Interface Anal. **21**, 165–176 (1994).